ADVANCED FUNCTIONAL MATERIALS

FULL PAPER

DOI: 10.1002/adfm.200700065

Correlations between Percolation Threshold, Dispersion State, and Aspect Ratio of Carbon Nanotubes

By *Jing Li*, *Peng Cheng Ma*, *Wing Sze Chow*, *Chi Kai To*, *Ben Zhong Tang*, and *Jang-Kyo Kim**

Critical factors that determine the percolation threshold of carbon nanotube (CNT)-reinforced polymer nanocomposites are studied. An improved analytical model is developed based on an interparticle distance concept. Two dispersion parameters are introduced in the model to correctly reflect the different dispersion states of CNTs in the matrix—entangled bundles and well-dispersed individual CNTs. CNT–epoxy nanocomposites with different dispersion states are fabricated from the same constituent materials by employing different processing conditions. The corresponding percolation thresholds of the nanocomposites vary over a wide range, from 0.1 to greater than 1.0 wt %, and these variations are explained in terms of dispersion parameters and aspect ratios of CNTs. Important factors that control the percolation threshold of nanocomposites are identified based on the comparison between modeling data and experimental results.

1. Introduction

Carbon nanotubes (CNTs) have attracted much attention as the electrical conducting filler for conducting polymer nanocomposites, as they are capable of dissipating electrostatic charges and shielding devices from electromagnetic radiation. Significant research efforts have been directed toward the synthesis and characterization of CNT–polymer nanocomposites to further improve their functional and mechanical properties and thus to identify other potential applications. The percolation threshold of CNT-reinforced polymer nanocomposites is much lower than for composites containing conventional conducting fillers, such as metallic particles, carbon black, or carbon fibers, because of the high aspect ratio and high specific surface area of CNTs. The percolation threshold of carbon black ranges normally from approximately 3 to 15 wt %, and the threshold for metallic powders is often above 60 wt %, which is at least one order of magnitude higher than for CNTs.

To date, there has been no apparent consensus on the percolation threshold values for CNTs. For example, the values reported in the literature for typical CNT–epoxy nanocomposites vary from 0.002 to over 4 wt %[1–9] depending on the type of CNTs and the processing techniques used to produce the nanocomposites. Many different CNT dispersion techniques have been employed, including sonication, ball milling, shear mixing, and the use of dispersants or surfactants, along with different functionalization methods such as oxidation, amino-functionalization, silane-functionalization, and polymer grafting.[10–13] The effects of several processing parameters, such as shear rate, stirring temperature, curing conditions, and applied external electric field, on the electrical properties of nanocomposites have also been studied.[1,2] The large variation in the reported percolation threshold values indicates that the dispersion states and other properties of CNTs affected by different processing conditions are important in determining the electrical properties of CNT–polymer nanocomposites.

For short carbon-fiber- or graphite-nanoplatelet (GNP)-reinforced polymer nanocomposites, the aspect ratio of the filler is the most dominant factor according to experimental and theoretical models.[14,15] In our previous study,[15] an analytical model was developed based on the average interparticle distance concept to predict the percolation threshold of conducting polymer composites containing disc-shaped graphite nanoparticles with high aspect ratios. The parametric study suggested that the thickness and diameter of the fillers were important factors that determined the percolation threshold of conducting nanocomposites. Several theoretical studies have also focused on the percolation threshold of CNT-reinforced polymer nanocomposites, including an excluded volume approach and a numerical simulation,[16–18] which were originally proposed for carbon-fiber-reinforced polymer nanocomposites.[19] The CNT agglomerates were modeled as close-packed bundles of CNT cylinders with large diameters and identical lengths. This approximation is a simplification of the experimentally observed CNT agglomerates and does not take into consideration the waviness and 3D entanglement of CNTs. A two-parametric model was also proposed that considers the CNT agglomerates as spherical inclusions to study the effect of CNT agglomeration on the elastic properties of CNT-reinforced composites.[20]

[*] Dr. J.-K. Kim, J. Li, P. C. Ma, W. S. Chow, C. K. To
Department of Mechanical Engineering
The Hong Kong University of Science and Technology
Clear Water Bay, Kowloon, Hong Kong (P.R. China)
E-mail: mejkkim@ust.hk
B. Z. Tang
Department of Chemistry
The Hong Kong University of Science and Technology
Clear Water Bay, Kowloon, Hong Kong (P.R. China)

© 2007 WILEY-VCH Verlag GmbH & Co. KGaA, Weinheim

LGES 1037
LGES v. MRD
IPR2024-01012

This paper is part of a larger project on the development of conducting polymer composites containing nanoscale fillers, such as GNPs and CNTs. In this paper, critical parameters are identified based on theoretical analysis and experimental results that determine the percolation threshold of CNT-reinforced polymer nanocomposites. A new approach is devised to model the effect of the CNT dispersion state and aspect ratio on percolation threshold, which is verified by experimental measurements.

2. Experimental Measurements

2.1. Size Distributions and Morphologies of CNT Agglomerates

Figure 1 shows the histograms of CNT agglomerate sizes measured by a particle size analyzer. In this study, size is defined as the 'effective diameter of CNT agglomerates' and is given as the corresponding mean value ± one standard deviation after dispersion in a solvent by using the methods described in Table 1; the agglomerate size was measured before the CNTs were embedded in an epoxy resin. When comparing the CNT agglomerates dispersed according to Condition A to those CNTs processed according to Condition B, the mean particle size decreased from 136 μm for the as-received CNTs to 34.7 μm, suggesting breakage of CNT agglomerates by ultrasonication. When using Condition C for dispersion, the mean particle size was further reduced to 290 nm and exhibited a bimodal distribution with two peaks located at 214 and 412 nm. Under Condition D, the mean size was reduced to 110 nm with a more distinct bimodal distribution, and the corresponding peak values were 58 and 342 nm. It is noted that the number fraction of particles in the second peak was very small compared to the fraction of particles found in the first peak

Table 1. Processing methods (Conditions A, B, C, and D) used to disperse CNTs and the corresponding percolation thresholds.

Condition	Dispersion method	Percolation threshold [wt%/vol%]
A	As-received CNTs + epoxy Shear mixing for 30 min at 3000 rpm	0.4/0.26
B	CNTs dispersed by ultrasonication for 1 h in acetone + epoxy Ultrasonication for 2 h at 60 °C	0.1/0.06
C	UV/ O_3 treatment of CNT for 1 h and ultrasonication for 2 h in acetone + epoxy Shear mixing for 30 min at 3000 rpm	0.25–0.3/0.16–0.19
D	CNTs were ball milled for 2 h, ultrasonicated in toluene for 1 h, and UV/O_3 treated for 2 h, followed by silane treatment [13] + epoxy Ultrasonicated for 2 h at 60 °C	No percolation

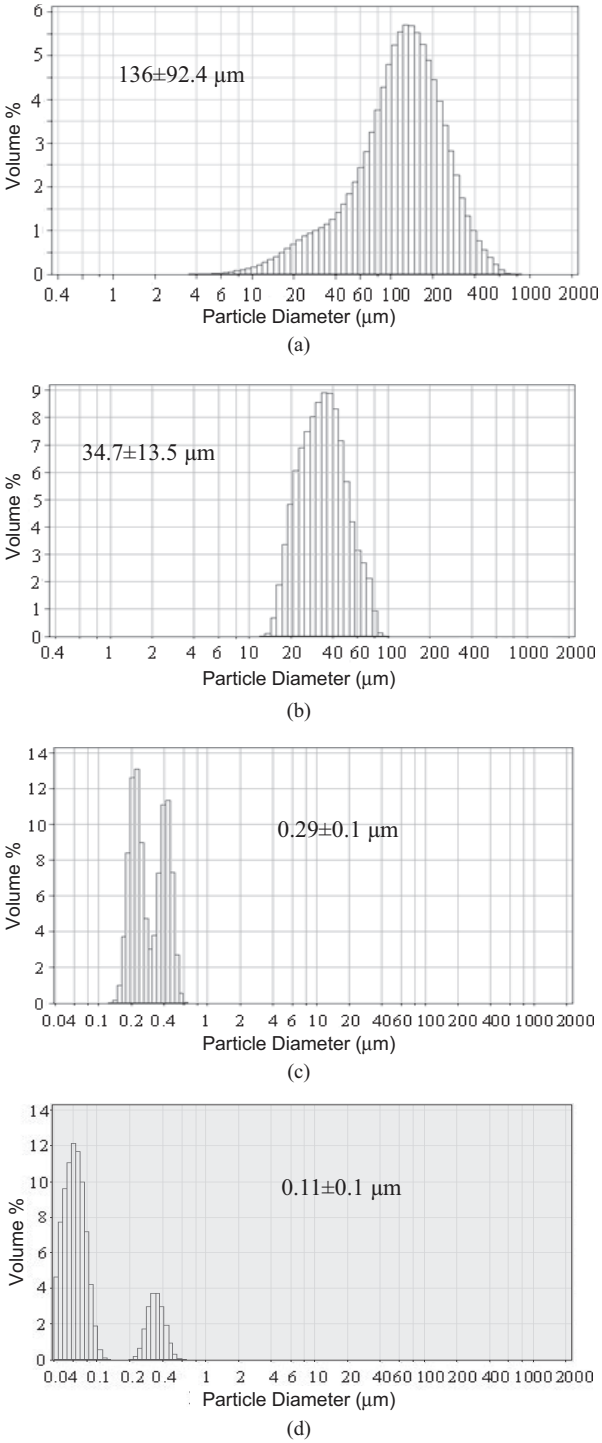


Figure 1. Size distributions of CNT agglomerates produced according to a) Condition A, b) Condition B, c) Condition C, and d) Condition D, before being embedded in an epoxy resin.

© 2007 WILEY-VCH Verlag GmbH & Co. KGaA, Weinheim

16163928, 2007, 16, Downloaded from https://advanced.onlinelibrary.wiley.com/doi/10.1002/adfm.200700065 by University Of Massachusetts, Wiley Online Library on [09/06/2025]. See the Terms and Conditions (https://onlinelibrary.wiley.com/terms-and-conditions) on Wiley Online Library for rules of use; OA articles are governed by the applicable Creative Commons License

ADVANCED FUNCTIONAL MATERIALS

FULL PAPER

1616302X, 2007, 17, Downloaded from https://onlinelibrary.wiley.com/doi/10.1002/adfm.200700065 by University Of Massachusetts, Wiley Online Library on [09/06/2025]. See the Terms and Conditions (https://onlinelibrary.wiley.com/terms-and-conditions) on Wiley Online Library for rules of use; OA articles are governed by the applicable Creative Commons License

(99.88 % vs. 0.12 %). We suspect, however, that some particles were even smaller than 40 nm, which is the lowest limit detectable by the particle size analyzer used in this study.

The corresponding transmission electron microscopy (TEM) images (Fig. 2) of the CNT agglomerates obtained by using the above processing conditions displayed the nanoscale disentanglement of CNTs. There was a systematic reduction in the packing density or 'degree of entanglement' that occurred in the order Condition A, Condition B, Condition C, Condition D. The CNTs processed according to Condition A were so tightly entangled that the localized CNT content was much higher than for CNTs dispersed by the other conditions. If the composites were made from these CNTs, there might be isolated CNT-rich regions along with a vast majority of composite volume that would be largely un-reinforced or resin-rich. Conditions B, C, and D led to disentangled CNTs, as shown in Figure 2, with an associated reduction in the size distribution of CNT agglomerates (Fig. 1). All of these observations suggest that under Conditions B, C, and D, the CNT agglomerates were disentangled, and the corresponding aspect ratios decreased because of the gradual breakage of CNTs.

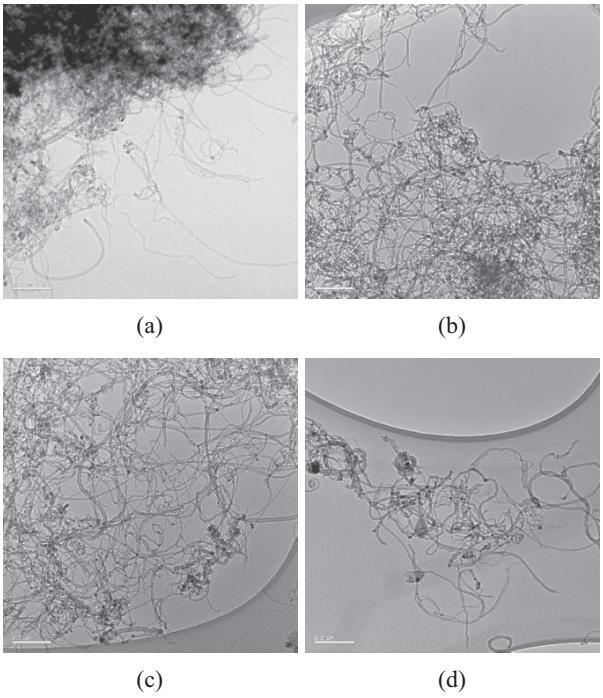


Figure 2. TEM images of CNT agglomerates dispersed according to Conditions A, B, C, and D described in Table 1 (scale bar = 0.2 μm).

2.2. Morphologies of CNT–Epoxy Nanocomposites

The fractured surface morphologies of 0.1 wt % CNT–epoxy nanocomposites shown in the scanning electron microscopy (SEM) images in Figure 3 provide some insight into the nanoscale dispersion state of CNTs. Large CNT agglomerates were obtained from Conditions A and B, whereas these agglomerates were almost completely absent for the composites produced by Conditions C and D. For Condition C, although entangled CNT bundles were not observed, the dispersion state was not as uniform as for Condition D. These observations are in agreement with a reduction in agglomerate size (Fig. 1) and disentanglement (Fig. 2).

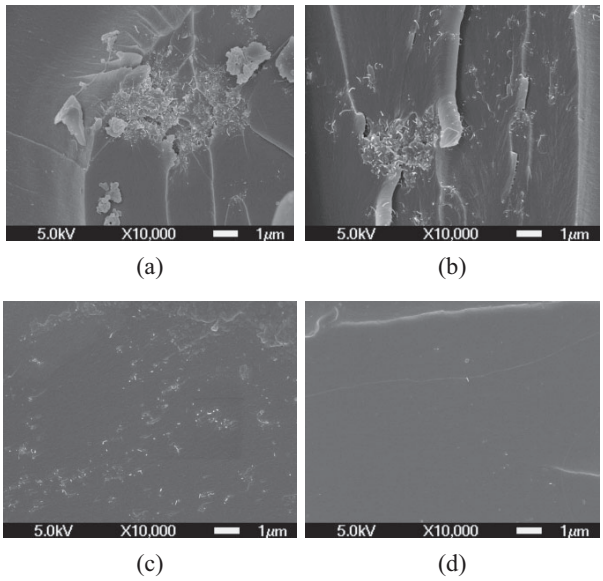


Figure 3. SEM images of 0.1 wt % CNT–epoxy nanocomposites dispersed according to Conditions A, B, C, and D described in Table 1 (scale bar = 1 μm).

Figure 4 presents the micro- and macroscopic morphologies of 0.05 wt % CNT–epoxy nanocomposites, illustrating the overall distributions of CNTs in the matrices obtained from different processing conditions. For Condition A (Fig. 4a and e), several isolated large CNT agglomerates were observed, which covered only a small portion of the total area because the CNTs were entangled very tightly and the CNT agglomerates were present in a small localized area (consistent with Fig. 2a). For Condition B (Fig. 4b and f), the CNT agglomerates covered a larger area, indicating that the entanglement of CNTs became much looser than under Condition A because of the added ultrasonication step (consistent with Fig. 2b), which allowed for the easier formation of conducting networks. For Condition C, although the disentanglement of CNTs was satisfactory at the nanoscale (Figs. 2c and 3c) and a large area was covered by CNTs, the corresponding micro- and macroscopic dispersion states (Fig. 4c and g) were poorer than for Condition B. It is believed that the disentangled CNTs, without sufficient surface functional groups, tend to re-agglomerate because of van der Waals and Coulomb attractions. A proper surface treatment, such as the treatment supplied by Condition D, can introduce electrostatic repulsion and achieve a stable CNT dispersion in the epoxy. The re-agglomeration process is known to

 © 2007 WILEY-VCH Verlag GmbH & Co. KGaA, Weinheim

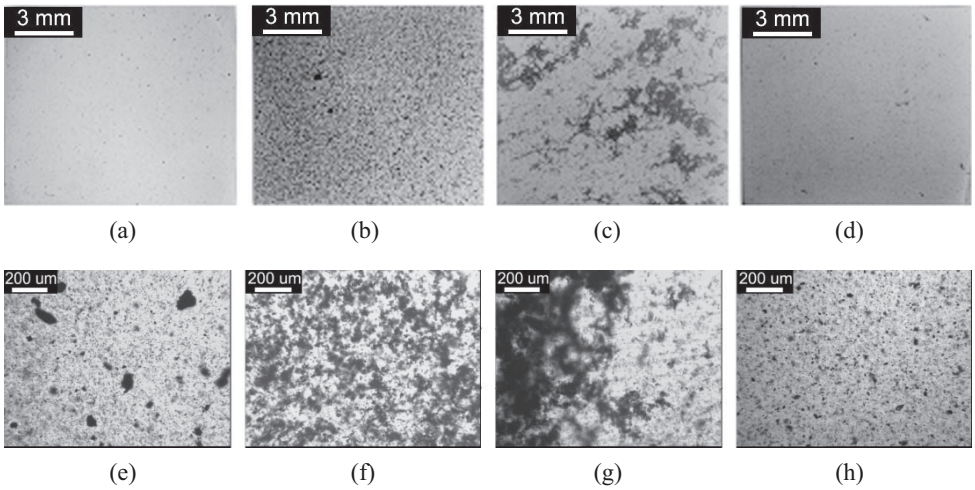


Figure 4. Transmission mode optical microscopy images of 0.05 wt % CNT–epoxy nanocomposites for Conditions A through D at different magnifications.

be time-dependent,[21] and thus for Condition C, it happened most likely during the degassing process when the mixture was held for several hours at 80 °C. Under Condition D, the size of the CNT agglomerates was the smallest among all of the conditions studied (Fig. 1d), and the CNTs exhibited satisfactory disentanglement (Figs. 2d and 3d), leading to barely visible agglomerates under the optical microscope (Fig. 4d and h). It should be noted here that the composite samples prepared according to Conditions A and D were almost transparent although the sample processed according to Condition D was slightly darker than when Condition A was followed (Fig. 4a and d). However, the reasons for these observations are totally different for the two conditions: the transparency of the Condition A sample was a reflection of the majority of the area being unfilled because of the tight entanglement of CNTs, whereas the transparency of the Condition D sample arose from the very good dispersion of CNTs at both the nano- and microscopic scales.

The dispersion of CNTs in polymer matrices has been studied extensively in recent years. Judging from the above explanations on the morphologies of CNT–epoxy nanocomposites, it is obvious that dispersion states of CNTs in the epoxy matrix can be totally different depending on the magnification or scale. It should be noted, however, that the previous studies often confusingly used the term 'uniform' dispersion or 'good' dispersion to describe the CNT dispersion states without any distinction between those dispersions observed under different magnifications. It is important to clearly define the dispersion of CNTs based on the different scales before any related discussion is made. For conventional composites, 'dispersion' is defined as an '*even distribution*' of fine particles in a matrix medium. In contrast, for CNT–polymer nanocomposites, 'dispersion' has two aspects: i) '*disentanglement*' of CNT bundles or agglomerates, which is a 'nanoscopic dispersion', and ii) '*uniform distribution*' of individual CNTs or their agglomerates throughout the nanocomposites, which is more of a 'micro- and macroscopic dispersion'.

2.3. Electrical Conductivities

The electrical conductivities of the nanocomposites prepared by using the four different conditions are presented in Figures 5 and 6, and the corresponding percolation thresholds determined from the DC conductivity plots are summarized in Table 1. The DC electrical conductivity varied significantly depending on the processing conditions. The percolation threshold of the composite prepared by Condition A was high (0.4 wt %) because the large, tightly entangled, CNT agglomerates made it difficult to form conducting networks at low filler contents. The sample prepared by Condition B had the lowest percolation threshold, 0.1 wt %, because of the loosely entangled and uniformly distributed CNT agglomerates. The mi-

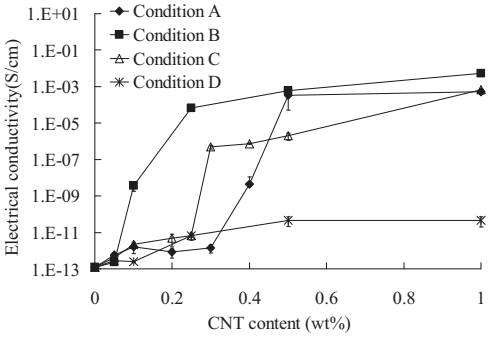


Figure 5. DC electrical conductivities of nanocomposites as a function of CNT content.

© 2007 WILEY-VCH Verlag GmbH & Co. KGaA, Weinheim

16163028, 2007, 16, Downloaded from https://advanced.onlinelibrary.wiley.com/doi/10.1002/adfm.200700065 by University Of Massachusetts, Wiley Online Library on [09/06/2025]. See the Terms and Conditions (https://onlinelibrary.wiley.com/terms-and-conditions) on Wiley Online Library for rules of use; OA articles are governed by the applicable Creative Commons License

ADVANCED FUNCTIONAL MATERIALS

16163028, 2007, 17, Downloaded from https://onlinelibrary.wiley.com/doi/10.1002/adfm.200700065 by University Of Massachusetts, Wiley Online Library on [09/06/2025]. See the Terms and Conditions (https://onlinelibrary.wiley.com/terms-and-conditions) on Wiley Online Library for rules of use; OA articles are governed by the applicable Creative Commons License

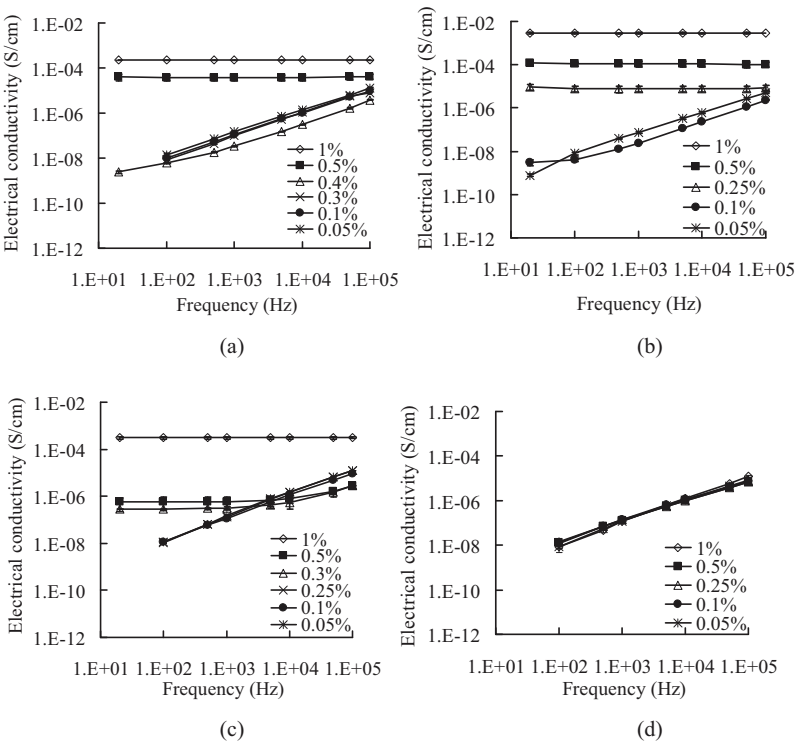


Figure 6. Frequency dependence of the AC conductivity of nanocomposites produced by a) Condition A, b) Condition B, c) Condition C, and d) Condition D.

croscopic distribution of CNTs obtained from Condition C was the least uniform even though the nanoscopic disentanglement of CNTs was quite satisfactory (Fig. 3c), resulting in a moderate percolation threshold value (0.25–0.3 wt %). Although CNTs from Condition D exhibited the best dispersion state at both the nano- and microscales, no apparent percolation threshold was observed, even with a 1 wt % CNT content. A plausible explanation is that the CNTs were severely damaged and broken into very short pieces during the combined ball-milling, ultrasonication, and silanizing treatment steps,[13] resulting in a large reduction in the CNT aspect ratio. It follows then that the very low aspect ratio observed for the CNTs obtained from Condition D and the silane coating, which acted as the physical barrier to electrical conduction, became the predominant factors that controlled the entire electrical conduction behavior of the nanocomposite. This result suggests that if the CNT aspect ratio is too low, the formation of conduction networks requires a very high CNT content, no matter how the CNT dispersion state is; this result is also seen for other conventional conducting polymers containing short carbon fibers or carbon black.

Figure 6 shows the frequency dependency of AC conductivities of nanocomposites with varying CNT contents, which indicates the overall connectivity of the conducting network. It is interesting to note that below the percolation threshold, the AC conductivity increased linearly with frequency because of dielectric loss. When the CNT content was approximately in the percolation transition range where both isolated CNTs and tunneling conduction pathways existed in the composites, the AC electrical conductivity became a constant up to a certain frequency value, above which the conductivity increased linearly with frequency. Above the percolation threshold, the ohmic conduction pathway took over, and the AC conductivity remained constant over the entire frequency range studied. The percolation threshold values determined were in agreement with those obtained from the DC conductivity measurements (as listed in Table 1).

3. Theoretical Analysis

3.1. Improved Interparticle Distance (*IPD*) Model with Two Descriptive Dispersion Parameters

Based on the average *IPD* approach,[15] the composite is divided into cubic elements with length L, each containing one conductive particle in the center, and the total number of cubic elements is equal to the total number of particles. Here, the conductive particles could be either a single CNT or a bundle of CNTs, depending on the dispersion state

$$\frac{V_{total}}{L^3} = \frac{V_{filler}}{n\,V_{CNT}} \tag{1}$$

where V_{total} is the total volume of composites, V_{filler} is the total volume of filler, V_{CNT} is the volume of the individual CNT, and n is the number of CNTs in an agglomerate (i.e., $n = 1$ in the case of a perfect dispersion). The conducting fillers were assumed to be homogeneously distributed within the matrix and perfectly bonded to the polymer. Two extreme cases were considered for the dispersion of CNTs within the polymer matrix: i) all of cylindrical CNTs are perfectly dispersed in the matrix (Fig. 7a) and ii) all of the CNTs are present in the form of agglomerates (Fig. 7b). Suppose that the individual CNT is cylindrical with length l and diameter d, and the CNT agglomerate exists in the form of a sphere of diameter D with a higher concentration of CNTs than the average filler content. For a perfect dispersion where all CNTs are present in the form of individual cylinders, the filler volume fraction, P, is given by[15]

$$P = \frac{V_{filler}}{V_{total}} = \frac{V_{CNT}}{L^3} = \frac{\frac{\pi d^2 l}{4}}{[\langle \cos^2\theta \rangle \cdot (l + IPD)]^3} \tag{2}$$

where θ represents the angle between the CNT and the direction of preferred orientation, and the angular brackets $\langle\rangle$

© 2007 WILEY-VCH Verlag GmbH & Co. KGaA, Weinheim

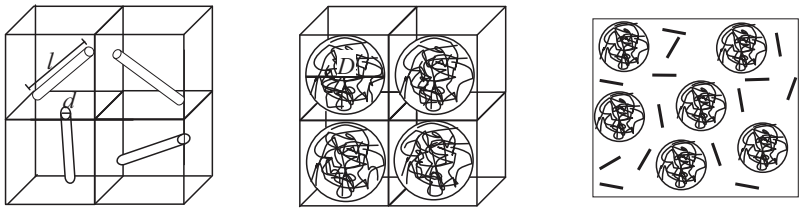


Figure 7. Cartoons of CNT-reinforced polymer nanocomposites containing a) perfectly dispersed cylindrical CNTs, b) CNTs all in the form of agglomerates, and c) a mixture of individual CNTs and agglomerates.

denote the orientation average. For a 3D random distribution,[22]

$$\langle \cos^2\theta \rangle = \frac{1}{3} \tag{3}$$

When *IPD* is equal to or less than 10 nm, electron hopping occurs, resulting in a rapid increase in the electrical conductivity of the composite, according to the tunneling mechanism,[23] and the filler content P becomes the percolation threshold P_c. Thus, $IPD = 10$ nm was taken as the criterion for the calculation of percolation thresholds. As the CNT length l is much longer than 10 nm, $l >> IPD$. Thus, combining Equations 2 and 3 gives

$$P_c \approx \frac{\frac{\pi d^2 l}{4}}{(\frac{1}{3}l)^3} = \frac{27\pi d^2}{4l^2} \tag{4}$$

Conversely, if all CNTs are present as agglomerates, P_c is given by

$$P_c = \frac{V_{filler}}{V_{total}} = \frac{nV_{CNT}}{L^3} \tag{5}$$

To understand how the dispersion state and aspect ratio of CNTs affect the percolation threshold of nanocomposites, two descriptive dispersion parameters are introduced: ε is the localized volume content of CNTs in an agglomerate, and ξ is the volume fraction of agglomerated CNTs

$$\varepsilon = \frac{nV_{CNT}}{\frac{\pi D^3}{6}} \quad (P < \varepsilon < 1) \tag{6}$$

$$\xi = \frac{\sum_{i=1}^{\frac{V_{total}}{L^3}} n_i V_{CNT}}{V_{filler}} \quad (\text{when } n_i \geq 2)\ (0 < \xi < 1) \tag{7}$$

A higher ε value corresponds to more tightly entangled CNTs in an agglomerate, and thus the CNT agglomerates cover a smaller area on the microscopic scale (Fig. 4). The highest value of ε is 1, which corresponds to the state where CNT agglomerates are closely packed such that no polymer matrix is able to penetrate into the localized area. Meanwhile, a higher ξ means that the portion of CNTs in the form of agglomerates is higher, indicating that fewer individually dispersed CNTs exist on the nanoscale (Fig. 3). The highest value of ξ is 1, which is the state where all CNTs present are agglomerated. Contrastingly, in the case of a perfect dispersion, no agglomerated CNTs exist (at the lowest value, $\xi = 0$), and the localized CNT concentration is the same as the entire nanocomposite (at the lowest value, $\varepsilon = P$). The upper limits, $\varepsilon = 1$ and $\xi = 1$, are undesirable, whereas the lower limits, $\varepsilon = P$ and $\xi = 0$, are favorable for achieving an ultralow percolation threshold for the nanocomposites. It should be noted that ε and ξ describe only the 'degree of CNT entanglement', which is defined as the 'nanoscopic dispersion' in two different ways: i) ε describes how tight the entanglement is and ii) ξ presents how many individual CNTs are entangled in an agglomerate. A nonuniform distribution was not specifically considered in this model because the overall distribution was assumed to be homogeneous. Incorporating Equation 6 into Equation 5 and considering $D >> IPD$ at the percolation threshold, we obtained a simplified equation that depicts the percolation thresholds of nanocomposites with all CNTs in the agglomerated form

$$P_c = \frac{nV_{CNT}}{L^3} = \frac{\varepsilon\frac{\pi D^3}{6}}{(D+IPD)^3} \approx \frac{\varepsilon\pi}{6} \tag{8}$$

In practical nanocomposites, however, both individual, perfectly dispersed CNTs and CNT agglomerates exist (Fig. 7c). Thus, the percolation threshold of these nanocomposites can be expressed by

$$P_c = \frac{\xi\varepsilon\pi}{6} + \frac{(1-\xi)27\pi d^2}{4l^2} \tag{9}$$

3.2. Parametric Study

Parametric studies were conducted to evaluate the effect of the two dispersion parameters, ε and ξ, and the aspect ratio of CNTs on the percolation threshold of CNT-reinforced polymer nanocomposites. Figure 8 presents the percolation thresholds predicted based on Equation 9, where the two dispersion parameters were varied simultaneously.

We see that for a CNT aspect ratio of 200 (Fig. 8b), the percolation threshold would change three orders of magnitude when the two dispersion parameters, ε and ξ, are varied simultaneously from 0.01 to 0.3. Similarly, when the CNT aspect ratio is 2000 (Fig. 8a), the percolation threshold would change four orders of magnitude for the same range of dispersion parameters. It is interesting to note that when there is a sufficient number of entangled CNTs, approximately $\varepsilon \geq 0.1$ and $\xi \geq 0.1$,

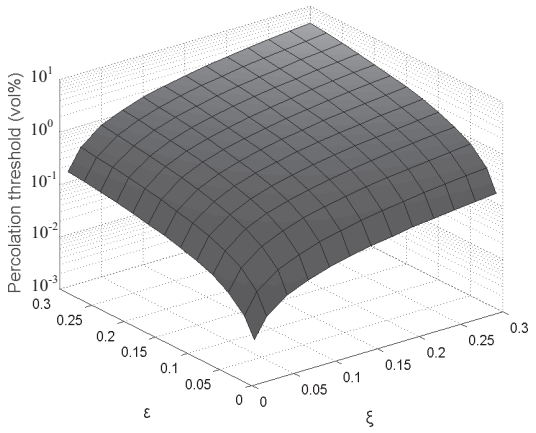
© 2007 WILEY-VCH Verlag GmbH & Co. KGaA, Weinheim

16163028, 2007, 16, Downloaded from https://advanced.onlinelibrary.wiley.com/doi/10.1002/adfm.200700065 by University Of Massachusetts, Wiley Online Library on [09/06/2025]. See the Terms and Conditions (https://onlinelibrary.wiley.com/terms-and-conditions) on Wiley Online Library for rules of use; OA articles are governed by the applicable Creative Commons License

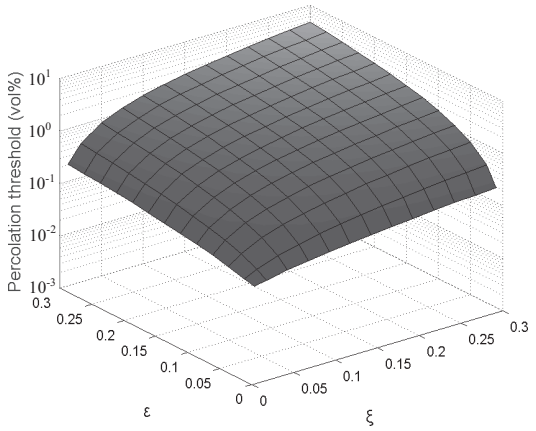
ADVANCED FUNCTIONAL MATERIALS

FULL PAPER

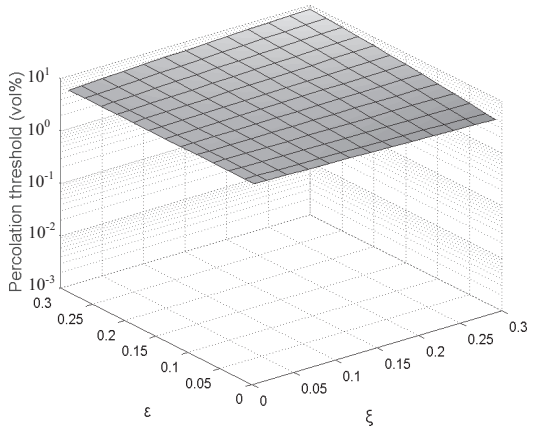
1616302X, 2007, 17, Downloaded from https://onlinelibrary.wiley.com/doi/10.1002/adfm.200700065 by University Of Massachusetts, Wiley Online Library on [09/06/2025]. See the Terms and Conditions (https://onlinelibrary.wiley.com/terms-and-conditions) on Wiley Online Library for rules of use; OA articles are governed by the applicable Creative Commons License



(a) Aspect ratio=2000



(b) Aspect ratio=200



(c) Aspect ratio=20

Figure 8. Effect of the dispersion parameters, ε and ξ, on the percolation threshold of CNT-reinforced polymer nanocomposites for aspect ratios a) $l/d = 2000$, b) $l/d = 200$ and c) $l/d = 20$.

Figure 8a and b become almost identical above the contour value of $P_c = 0.1$ vol %. These observations indicate that when the CNT aspect ratio is high, greater than about 200 for example, the CNT dispersion parameters, ε and ξ, determine the percolation threshold. The variation of P_c below the contour $P_c = 0.1$ vol % (Fig. 8a and b) also indicates that if the aspect ratio were increased from 200 to 2000, the percolation threshold would be reduced only when the CNTs were successfully disentangled (i.e., both ε and $\xi \leq 0.1$). In order to obtain an ultralow percolation threshold on the order of 10^{-3} vol %, both a very high aspect ratio and sufficient disentanglement of CNTs are required (Fig. 8a). For example, there were reports of ultralow percolation thresholds in the range of 0.0021–0.0039 wt % for epoxy nanocomposites containing as-grown, aligned, disentangled, relatively straight, high-aspect-ratio, multiwalled CNTs[1,3] and 0.0052–0.0085 vol % for epoxy nanocomposites containing well-dispersed, relatively straight, single-walled CNTs.[9]

When the aspect ratio is reduced to 20, the percolation threshold jumps to 1–10 vol % regardless of the dispersion states of CNTs, indicating that the aspect ratio becomes the predominant factor. It should be noted that an aspect ratio of 20 and a percolation threshold of 1–10 vol % are typical of some short carbon-fiber-reinforced polymer composites. It was found for a CNT–epoxy nanocomposite[8] that when the CNT aspect ratio was reduced from 417 to 83 and 8.3, the corresponding percolation threshold increased from 0.5 to 1.5 and >4 wt %, respectively. When ball milling was used to disperse CNTs,[4,5] the percolation threshold increased significantly because the ball milling process severely damaged CNTs, reducing their aspect ratio. In some cases (Condition D and [8]), a clear percolation threshold where the electrical behavior exhibits a sharp transition from insulating to electrically conducting could not be observed for the range of CNT loadings studied. A further increase in CNT content may allow one to observe a percolation threshold, but a CNT content that is too high is undesirable because the associated increase in the viscosity of the composite mixture would make processing extremely difficult.

The above parametric study can shed light onto how one can optimize the CNT processing conditions to reduce the percolation threshold of CNT–polymer nanocomposites. Both a high aspect ratio and disentanglement of CNTs on the nanoscale give rise to low dispersion parameters, ε and ξ, which are essential for achieving a low percolation threshold. However, many dispersion and functionalization techniques inevitably break the CNTs into smaller pieces, reducing the aspect ratio. It has been shown that broken CNTs with very low aspect ratios are the most detrimental to forming conducting networks even though they can give rise to good dispersions, as indicated for the samples processed according to Condition D. There exist critical aspect ratios of CNTs where the percolation threshold increases rapidly with decreasing aspect ratio depending on the degree of entanglement (i.e. dispersion parameters).

 © 2007 WILEY-VCH Verlag GmbH & Co. KGaA, Weinheim

4. Comparison of Modeling Data to Experimental Results

Figure 9 presents the effect of aspect ratio on the percolation thresholds predicted from Equation 9 with varying dispersion parameters, which are compared to the experimental data collected from the literature as well as from the results obtained in this study. The dispersion parameters, ε and ξ, were assumed to be identical to simplify the predictions. As expected, the higher the dispersion parameters, the higher the percolation threshold. At low aspect ratios, the percolation threshold decreased in a linear fashion with increasing aspect ratio. As the aspect ratio increased further, the percolation threshold gradually increased and reached a plateau. The transition occurred over a range of critical aspect ratios that depend on the dispersion parameters. For example, for $\varepsilon = \xi = 0.01$, the transition occurred in the aspect-ratio range 750–1500; and for $\varepsilon = \xi = 0.05$, it occurred between 100 and 300. For aspect ratios above the critical range, the percolation threshold became almost constant and independent of aspect ratio and varied only with the dispersion parameters (e.g., for a near-perfect dispersion $\varepsilon = \xi = 0.01$, the percolation threshold varied between 10^{-2} to 10^{-3} vol %, and for $\varepsilon = \xi = 0.05$, it increased from 0.1 to 1 vol %). The existence of this critical range of aspect ratios implies that there are predominant factors determining the percolation threshold, and the predominant factor changes from the aspect ratio to the degree of entanglement with increasing aspect ratio of CNTs. It is interesting to note that no matter how well the CNTs were disentangled, the percolation threshold could not be lowered below 1 vol % if the aspect ratio was lower than 50. This observation is consistent with the discussion in Section 3.2.

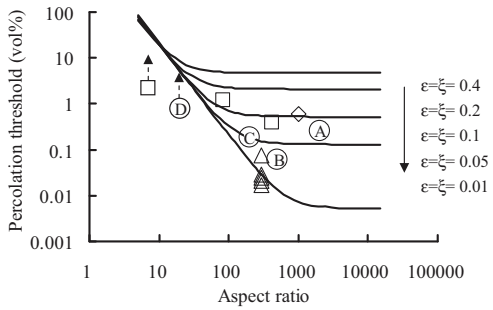


Figure 9. Effect of aspect ratio on the percolation threshold of CNT-reinforced polymer nanocomposites with varying dispersion states. Experimental data: Conditions A, B, C and D in the present study ○; □ [6]; □ [7] and □ [8].

A comparison to the experimental data further verified the applicability of this model. To identify the effect of the aspect ratio and dispersion states of CNTs on percolation threshold, percolation thresholds of composites made from similar constituent materials (i.e., epoxy and entangled multiwalled CNTs) were compared to predicted values. For the data shown in Figure 9, percolation threshold values reported in wt % were converted to the equivalent vol % by assuming a CNT density of 1.8 g cm^{-3}.[10] Because of the entanglement of CNTs within the polymer matrix, measuring the CNT lengths with any accuracy using a microscope was not a trivial task. It was thus not surprising that the aspect ratios of the CNTs after processing were not generally available in the literature except for the data found in [8]. In an effort to approximate the corresponding aspect ratios, three observations reported in the literature[6,7] and the current study, including the aspect ratios of as-received CNTs, the processing methods applied, and the TEM morphologies, were carefully analyzed. Ultrasonication and ball-milling techniques were found to reduce the length of CNTs,[11] while magnetic agitation, shear mixing, and chemical modification did not. The aspect ratios and the corresponding percolation thresholds obtained are listed in Table 2 along with the processing conditions applied for the dispersion of CNTs.

The comparisons given in Figure 9 indicate that the prediction, in general, agreed well with the experimental results with respect to the dispersion methods applied. The shear mixing (Condition A) did very little to disentangle CNT agglomerates, leading to dispersion parameters from 0.05 to 0.1. For Condition B, ultrasonication resulted in the disentanglement of CNT agglomerates to a certain extent while reducing the aspect ratio, which decreased the percolation threshold, yielding dispersion parameters ranging between 0.01 and 0.05. For Condition C, although the disentanglement was quite satisfactory, both of the dispersion parameters were about 0.05 because of the nonuniform distribution of CNTs. The experimental data taken from the literature were also analyzed based on the processing information. When CNTs were processed by mild oxidation, surfactant, ultrasonication, and two-roll milling,[6] the nanoscale dispersion was good, as confirmed by TEM and SEM images, and the dispersion parameter was approximately 0.01. For CNTs dispersed in methanol by magnetic stirring,[7,8] the percolation thresholds were relatively high due to the inadequate disentanglement of CNT agglomerates and gave rise to dispersion parameters near 0.1. The arrow with a dashed line in Figure 9 represents the results from Condition D of the

Table 2. Experimental data used in Figure 9 for various CNT–epoxy nanocomposites.

Reference	Aspect ratio	Processing method	Percolation threshold [vol%]
[6]	300	Oxidation, surfactant, sonication	0.017–0.077
[7]	1000	Magnetic agitation	0.6
[8]	417	Magnetic agitation	0.4
[8]	83	Magnetic agitation	1.2
[8]	8	Magnetic agitation	No percolation
Condition A	2000	Shear mixing	0.26
Condition B	500	Sonication	0.06
Condition C	200	UV/Ozone, sonication and shear mixing	0.19
Condition D	<50	Ball Milling, sonication, UV/Ozone, silane	No percolation

© 2007 WILEY-VCH Verlag GmbH & Co. KGaA, Weinheim

16163028, 2007, 16, Downloaded from https://advanced.onlinelibrary.wiley.com/doi/10.1002/adfm.200700065 by University Of Massachusetts, Wiley Online Library on [09/06/2025]. See the Terms and Conditions (https://onlinelibrary.wiley.com/terms-and-conditions) on Wiley Online Library for rules of use; OA articles are governed by the applicable Creative Commons License

ADVANCED FUNCTIONAL MATERIALS

FULL PAPER

16163028, 2007, 17, Downloaded from https://onlinelibrary.wiley.com/doi/10.1002/adfm.200700065 by University Of Massachusetts, Wiley Online Library on [09/06/2025]. See the Terms and Conditions (https://onlinelibrary.wiley.com/terms-and-conditions) on Wiley Online Library for rules of use; OA articles are governed by the applicable Creative Commons License

present study and from [8], where the aspect ratios of the CNTs used in these studies were too low to show obvious percolation for the CNT contents employed. The above explanations together with the experimental studies presented in Section 2 confirm the validity of the model presented here for establishing a correlation between the percolation thresholds of CNT–polymer nanocomposites, the corresponding aspect ratios, and the degree of CNT disentanglement.

5. Conclusions

Experimental and theoretical studies were used to identify critical factors that determine the percolation thresholds of CNT-reinforced polymer nanocomposites. CNT–epoxy nanocomposites with different dispersion states were produced by using four different processing conditions, and their electrical properties were characterized. Several techniques were employed to investigate the nano-, micro- and macroscopic dispersion states of CNTs in the matrix.

An improved model with two descriptive dispersion parameters was proposed to predict the percolation threshold of CNT nanocomposites based on average interparticle distances. We found that percolation thresholds varied from 0.1 wt % to >1 wt % with different processing techniques, which produced different nano-, micro- and macroscopic dispersion states and CNT aspect ratios. Furthermore, the critical factors determining the percolation threshold of CNT–polymer nanocomposites include i) the aspect ratio of CNTs, ii) disentanglement of CNT agglomerates on the nanoscale, and iii) the uniform distribution of individual CNTs or CNT agglomerates on the microscopic scale. The model formulated in this study can be used to establish the correlations between percolation threshold, dispersion state, and CNT aspect ratio. A parametric study was performed, which illustrated how one could optimize the CNT processing conditions to reduce the percolation threshold of CNT–polymer nanocomposites.

There is a critical value of the CNT aspect ratio, above which the two dispersion parameters become crucial while allowing the percolation threshold to vary several orders of magnitude. In contrast, below this value the percolation threshold increases rapidly with decreasing aspect ratio. To verify the applicability of the present model, comparisons were made between the predicted results and the experimental data collected from the literature and this study. Good agreement was obtained from comparing processing methods and dispersion parameters.

6. Experimental

Four different batches of CNT-reinforced epoxy nanocomposites with different dispersion states were fabricated by using four different processing conditions, as listed in Table 1. The composites were made from epoxy (Epon 828, supplied by Shell Chemical) and multiwalled CNTs and prepared by a chemical vapor deposition method with a purity of carbon content more than 95 wt % (supplied by Iljin Nanotech, Korea). The diameters and lengths ranged from 10 to 20 nm and from 10 to 50 μm, respectively. After the CNTs were dispersed in epoxy, the mixtures were degassed, and a curing agent, 1,3-phenylenediamine (mPDA, supplied by Sigma-Aldrich), was added to the mixture in the ratio of 14.5:100 by weight. The composite was molded into a flat plate and cured at 80 °C for 2 h, followed by post curing at 150 °C for 3 h.

The size distributions and morphologies of CNT agglomerations were characterized by using a particle size analyzer (COULTER LS 230) and a transmission electron microscope (JEOL 2010F), respectively. The dispersion states of CNTs on the fractured surfaces of nanocomposite were also examined with a scanning electron microscope (JEOL-6700F). The electrical conducting networks on the polished nanocomposite samples 0.4 mm thick were visualized using the transmission mode of an optical microscope.

DC conductivity of nanocomposites with varying CNT contents were measured based on the four-probe method using a resistivity/Hall measurement system (Bio-Rad HL5500PC). As the lowest limit of the electrical conductivity measured by using the resistivity/Hall measurement system was 10^{-8} S cm^{-1}, the electrical conductivity of nanocomposites lower than this limit was measured with a programmable curve tracer (Sony Tektronix 370A), whose lowest limit was 10^{-13} S cm^{-1}. AC conductivity of the nanocomposites was measured with a precision LCR meter (Hewlett Packard 4284A) in the frequency range of 20–10^5 Hz. Specimens were polished on both sides to a thickness of 1 mm, and silver paste was applied to minimize the contact resistance between the composite sample and the electrodes.

Received: January 15, 2007
Revised: April 23, 2007
Published online: September 5, 2007

[1] C. A. Martin, J. K. W. Sandler, M. S. P. Shaffer, M. K. Schwarz, W. Bauhofer, K. Schulte, A. H. Windle, *Compos. Sci. Technol.* **2004**, *64*, 2309.
[2] C. A. Martin, J. K. W. Sandler, A. H. Windle, M. K. Schwarz, W. Bauhofer, K. Schulte, M. S. P. Shaffer, *Polymer* **2005**, *46*, 877.
[3] J. K. W. Sandler, J. E. Kirk, I. A. Kinloch, M. S. P. Shaffer, A. H. Windle, *Polymer* **2003**, *44*, 5893.
[4] A. Moisala, Q. Li, I. A. Kinloch, A. H. Windle, *Compos. Sci. Technol.* **2006**, *66*, 1285.
[5] F. H. Gojny, M. H. G. Wichmann, B. Fiedler, I. A. Kinloch, W. Bauhofer, A. H. Windle, K. Schulte, *Polymer* **2006**, *47*, 2036.
[6] Y. J. Kim, T. S. Shin, H. D. Choi, J. H. Kwon, Y. C. Chung, H. G. Yoon, *Carbon* **2005**, *43*, 23.
[7] A. Allaoui, S. Bai, H. M. Cheng, J. B. Bai, *Compos. Sci. Technol.* **2002**, *62*, 1993.
[8] J. B. Bai, A. Allaoui, *Compos.: Part A* **2003**, *34*, 689.
[9] M. B. Bryning, M. F. Islam, J. M. Kikkawa, A. G. Yodh, *Adv. Mater.* **2005**, *17*, 1186.
[10] X. L. Xie, Y. W. Mai, X. P. Zhou, *Mater. Sci. Eng. R* **2005**, *49*, 89.
[11] J. Hilding, E. A. Grulke, Z. G. Zhang, F. Lockwood, *J. Dispersion Sci. Technol.* **2003**, *24*, 1.
[12] M. L. Sham, J. K. Kim, *Carbon* **2006**, *44*, 768.
[13] P. C. Ma, J. K. Kim, B. Z. Tang, *Carbon* **2006**, *44*, 3232.
[14] A. Celzard, E. McRae, C. Deleuze, M. Dufort, G. Furdin, J. F. Mareche, *Phys. Rev. B* **1996**, *53*, 6209.
[15] J. Li, J. K. Kim, *Compos. Sci. Technol.* **2007**, *67*, 2114.
[16] M. Foygel, R. D. Morris, D. Anez, S. French, V. L. Sobolev, *Phys. Rev. B* **2005**, *71*, 104 201.
[17] M. Grujicic, G. Cao, W. N. Roy, *J. Mater. Sci.* **2004**, *39*, 4441.
[18] Z. Ounaies, C. Park, K. E. Wise, E. J. Siochi, J. S. Harrison, *Compos. Sci. Technol.* **2003**, *63*, 1637.
[19] I. Balberg, N. Binenbaum, N. Wagner, *Phys. Rev. Lett.* **1984**, *52*, 1465.
[20] D. L. Shi, X. Q. Feng, Y. Y. Huang, K. C. Hwang, H. Gao, *J. Eng. Mater. Technol.* **2004**, *126*, 250.
[21] S. K. Mhetre, Y. K. Kim, S. B. Warner, P. K. Patra, P. Katangur, A. Dhanote, *Mater. Res. Soc. Symp. Proc.* **2004**, *788*.
[22] S. Chandrasekhar, *Liquid crystals*, Cambridge University Press, New York **1992**, Ch. 2.
[23] G. R. Fiuschau, S. Yoshikawa, R. E. Newnham, *J. Appl. Phys.* **1992**, *72*, 953.

 © 2007 WILEY-VCH Verlag GmbH & Co. KGaA, Weinheim